Integral Operations: a Reliable Prediction of Van Allen Belt Crossings

M. J. H. Walker[1]
SCISYS Deutschland GmbH, Darmstadt, Germany

J. B. Palmer[2]
Logica GmbH, Darmstadt, Germany

R. T. Southworth[3]
ESOC, Darmstadt, Germany

The Integral spacecraft, a Gamma, X-Ray and optical telescope operated by ESOC since 17/10/2002, is in a highly elliptical high inclination orbit and experiences a perigee passage through the Van Allen radiation belts every 3 sidereal days. As the high radiation experienced during these passages would damage the instruments, these are switched off. In addition to these periodic regular orbital events, there is significant long-term evolution of the orbital parameters, which also fundamentally affects the characteristics of the radiation belt crossings. To optimise the science return, it is necessary to be able to predict as accurately as possible when the instruments must be switched off, and when they can be safely switched back on. In this paper we explore the observation of a correspondence between the bi-annual geotail crossings, the eclipse seasons and the periodic variation in instrument activation and deactivation altitudes. The paper characterises the nature of these radiation belt passages and proposes a method of predicting their future trend as the orbit evolves. Our analysis will address the following:

Variation of Radiation belt entry and exit altitudes over time.

Precession of the orbital plane, in particular the rotation of the line of nodes and the corresponding effects on the bi-annual timing of eclipses and geotail crossings.

How the motion of the line of apsides impacts the belt crossing altitude.

Combination of all 3 of the above effects

The presented method and our findings could assist other missions by offering an optimisation strategy for science operations by predicting the evolution of radiation belt crossings and as a result, allow any protective measures to be implemented in time. In particular a methodology for data analysis and reduction is defined.

I. Introduction

THE **Integral** spacecraft, a mission to research gamma ray sources, was launched on 17/10/2002 into a highly elliptical near polar orbit with a period ('revolution') of 3 sidereal days. The scientific payload consists of a **gamma-ray spectrograph (SPI)**, a **gamma-ray imager (IBIS)**, **2 X-Ray imagers (JEMX 1 & 2)**, and an **optical monitor (OMC).** Since all these instruments are sensitive to and are impacted by high radiation levels, a **Radiation Environment Monitoring device (IREM)** has also been included as part of the payload. To protect the instruments from excessive radiation, they are commanded to a safe mode during periods of known high particle density, e.g. Van Allen Belt transits or when the **IREM** detects other high level radiation environments e.g. during solar flares.

Since the satellite is periodically outside ground station contact, use is made of on-board autonomy. This is governed by the spacecraft's Central Data Management Unit, which issues environmental information in the form of a telecommand packet to each instrument every 8 seconds. This packet includes, amongst other parameters, both

[1] Spacecraft Operations Engineer, ESA/ESOC HSO-OAI, mike.walker@scisys.de
[2] Space Flight Dynamics Engineer, ESA/ESOC Flight Dynamics, jpalmer@esa.int
[3] Spacecraft Operations Manager, ESA/ESOC HSO-OAI, rsouthwo@esa.int.

ground specified events such as predictions of the entry/ exit times of the radiation belts and eclipses, as well as three real-time radiation environment parameters directly from the **IREM**. The instruments react autonomously to the entry and exit times ensuring an orderly shut down of the instruments before the predicted entry into hostile environments. Without such orderly shutdowns, the instruments would undergo emergency shutdowns based on the **IREM** measurements and subsequently have to undergo lengthy reactivation procedures.
With this in mind, it's clear that the planned duration of scientific operations will be influenced by the accuracy of the Van Allen belt predictions. The more accurate the prediction, the closer to the predicted times and therefore the longer the instruments can be safely operated, avoiding emergency switch offs.

II. IREM and Instrument switch-off Logic

The on-board **IREM** device measures 15 radiation types, which are telemetered to ground as part of the science data, these are:

Parameter	Description	Particle types
TC1	E(p) > 20 MeV	Proton
S12	550 MeV > E(p) > 20 MeV	Proton
S13	120 MeV > E(p) > 20 MeV	Proton
S14	27 MeV > E(p) > 20 MeV	Proton
S15	34 Mev > E(p) > 20 MeV	Proton
TC2	E(p) > 39 MeV	Proton
S25	185 MeV > E(p) > 150 MeV	Ions
C1	50 MeV > E(p) > 40 MeV	Coincident Protons
C2	70 MeV > E(p) > 50 MeV	Coincident Protons
C3	120 MeV > E(p) > 70 MeV	Coincident Hard Protons
C4	E(p) > 130 MeV	Coincident Protons
TC3	E(e) > 0.5 MeV	Soft Electrons & Protons
S32	2.3 MeV > E(e) > 0.55 MeV	Soft Electrons & Protons
S33	90 MeV > E(p) > 11 MeV	Soft Proton
S34	30 MeV > E(p) > 11 MeV	Proton

Three radiation environment parameters, supplied by **IREM**, were selected to be distributed to the payload instruments:

1. **TC3** E(e) > 0.5 MeV Soft Electrons & Protons
2. **S14** 27 MeV > E(p) > 20 MeV Protons
3. **Dose**, a derived quantity based on the above values, plus dead-times.

Note that these are not the actual counts but a scaled measure of the environment (number of counts per 10 seconds divided by 256). The actual count rates would require more telemetry and command bandwidth, such accuracy is not required for the autonomous on-board protection.

Each instrument has 3 threshold settings for each of the above parameters which, when exceeded, will cause the unit to immediately switch to safe-mode. In practice, it has been observed that the **TC3** and **S14** parameters are the first to hit the limit, thus subsequent analysis has been based only around these quantities.

The thresholds specified for each instrument in terms of **IREM** counts are given below:

Instrument	**Electron Threshold TC3**	**Proton Threshold S14**
SPI	Not used	Not used
IBIS	200	60
JEM-X	64	20
OMC	2048	16

III. Orbit Geometry and Instrument Operations

Based on the **JEM-X** electron count threshold, the times when the counts exceeded or dropped below 64 **IREM** counts were selected as defining belt entry/exit. These times were recorded, and from them spacecraft altitudes were calculated.

Figure. 1 shows the resulting plot of the altitudes for threshold crossings during about 1150 orbital revolutions, i.e. about 9½ years. These values are taken for the purpose of defining Van Allen Belt **Entry and Exit altitudes**.

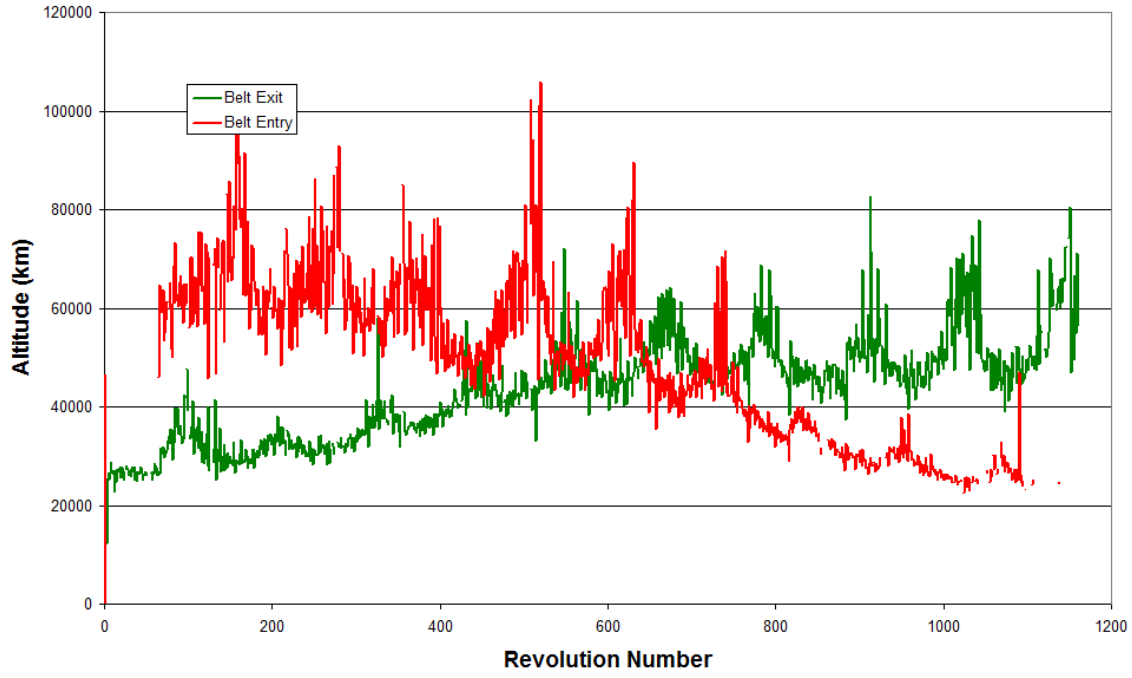

Figure. 1 Integral Radiation Belt Entry/Exit Altitudes

In trying to interpret the data, a first attempt was to separate the **Entry and Exit** curves and overlay them with a curve showing the eclipse season times, giving an indication of when the sun crosses the spacecraft orbital plane. The eclipses fall into two categories, pre and post perigee separated by about six months. The belt entry curve was overlaid with the post-perigee eclipse, and the belt exit with the pre-perigee eclipse. See figs. 2 & 3.

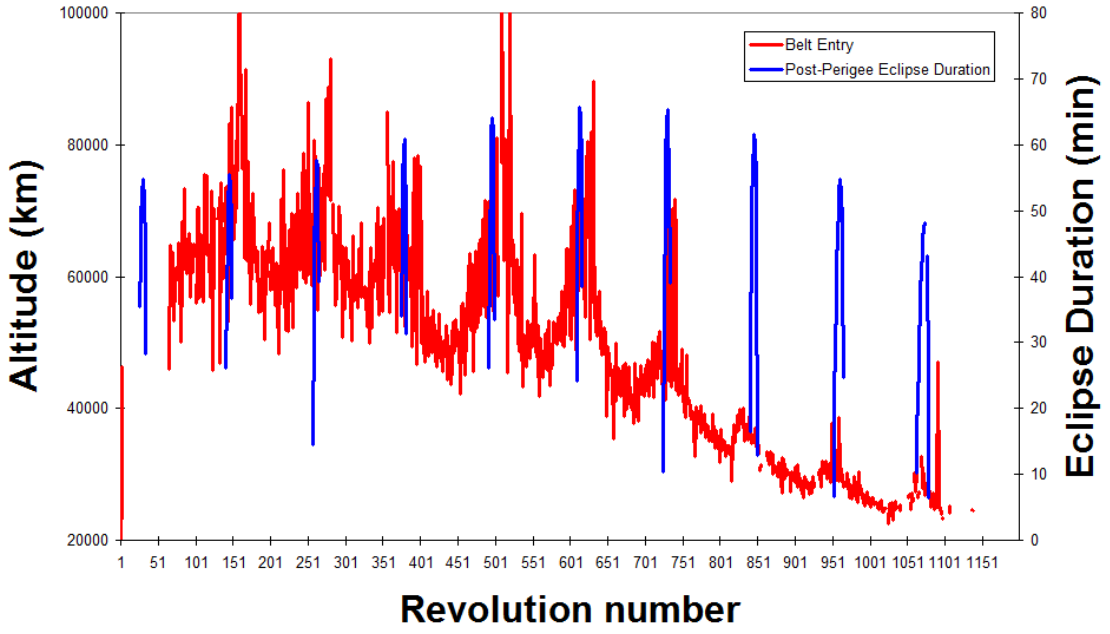

Figure. 2 Integral Radiation Belt Entry with post-perigee eclipse duration

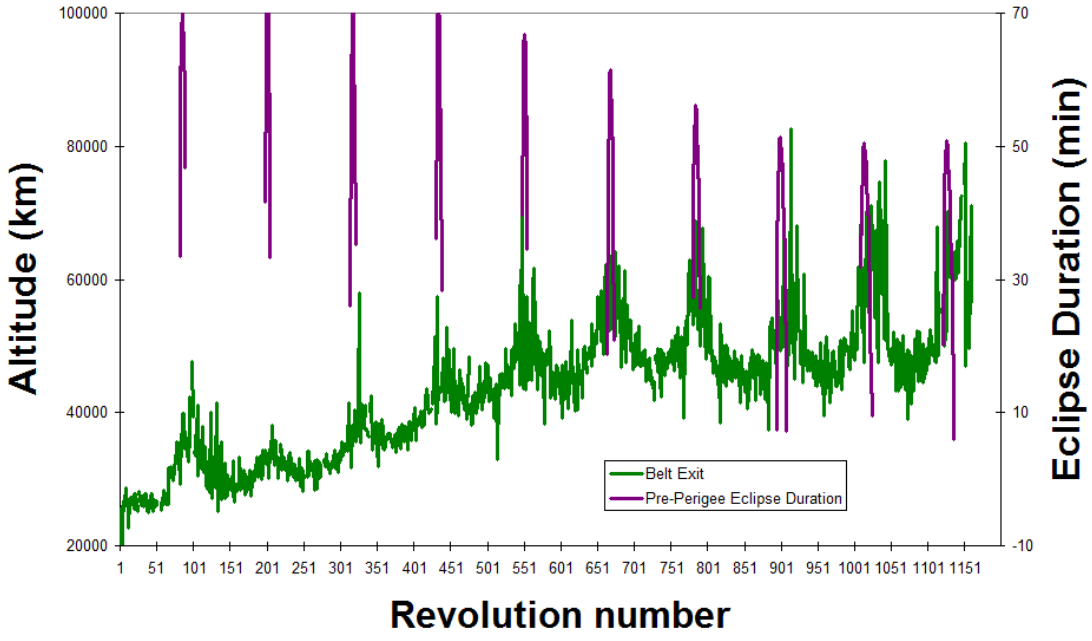

Figure. 3 Integral Radiation Belt Exit with pre-perigee eclipse duration

From figures 2 and 3, it is immediately apparent that the spikes on the belt entry/exit altitudes are correlated to the eclipse periods and therefore to the Sun crossing the orbital plane. It is at these times that the spacecraft is passing

behind the Earth through the geotail, a region where charged particles are concentrated and shaped much like a cometary tail, and hence the higher spacecraft altitude where this region is encountered.

Kalegaev, et al. and others model the geotail as a paraboloid, with the Earth at the focus, and the tail extending away from the sun. However, the data collected by **Integral** would indicate that the geotail does not extend directly away from the sun but may be curved, - again like a comet's tail, as in fig. 4. . This would agree with the east-west asymmetry of He^{2+} ions observed by Stubbs et al. The AP8-AE8 models of the radiation belts (Vette, Sawyer and Vette) do not include any parameters that could explain any such east-west asymmetry. However, more recent models of the magnetosphere include a dawn-dusk asymmetry (e.g. Tsyganenko), which may help to explain the effect.

Bearing in mind the orbital motion of the Earth it seems reasonable that the geotail is asymmetric; the diagram below indicates this well.

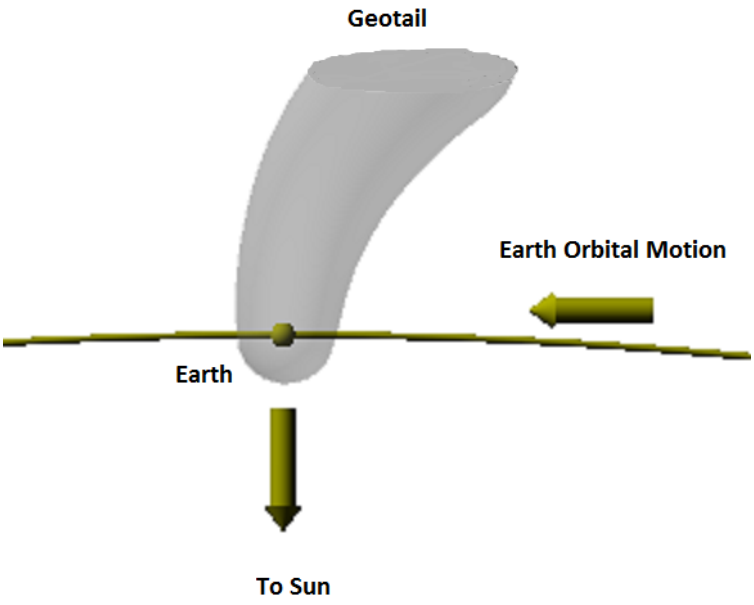

Figure 4 the Earth's geotail modelled as a curved paraboloid.

By overlaying the annual plots of the belt exit, aligning the plots using the maximum eclipse duration as a reference, the shearing of the belt exit curves can be shown more clearly as a repeatable effect see figure 5. Here the belt exit altitudes for the pre-perigee eclipse seasons for the years 2008 – 2012 are shown.

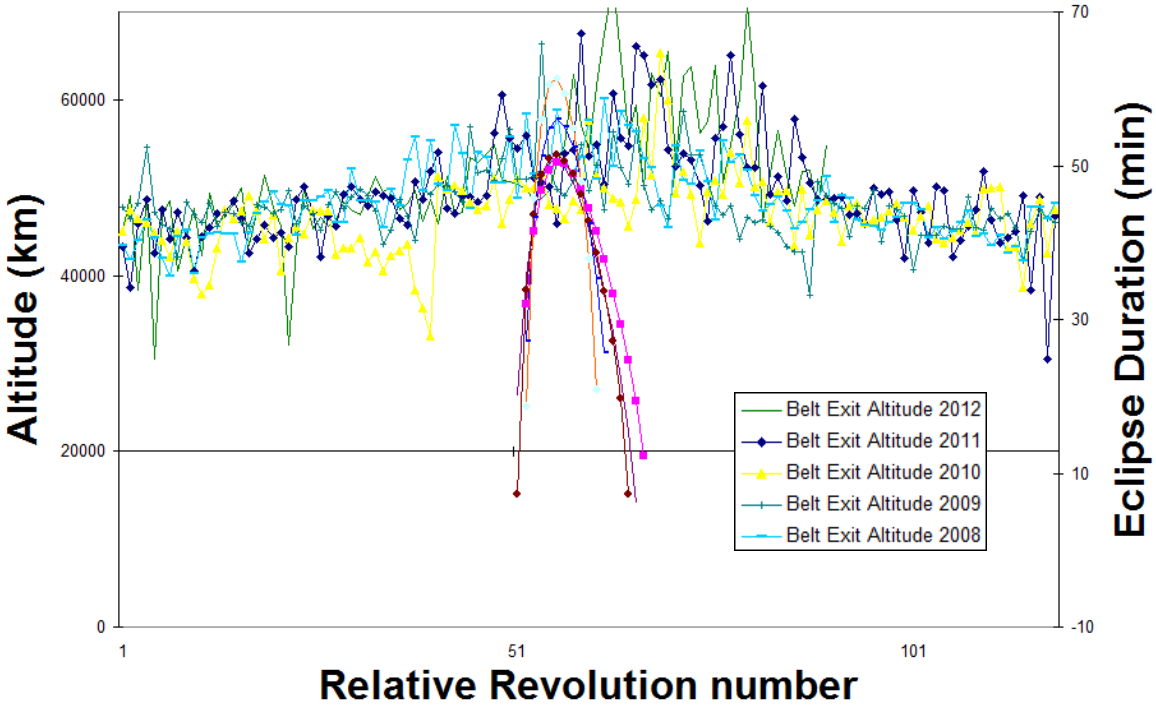

Fig. 5 Overlaid Belt exit altitudes with eclipses.

As input to the on-board autonomy, **Integral** requires specific times to be loaded with the predicted radiation belt entry & exit plus eclipse entry & exit times. These are known as "Critical Altitude Ascending", which defines the radiation belt exit, and "Critical Altitude Descending" defining the belt entry. Plots showing the history of these two parameters are given in figs. 6 & 7. It should be noted, that it is possible to commence payload activation operations before the belts exit, as it takes about 20 minutes to ramp up the high voltages, and in this time the radiation environment will naturally fall to tolerable levels.

It was not possible to apply a similar method to the radiation belt entry, due to the operational requirement to provide sufficient margin for manual intervention should a problem prevent the on-board autonomy from working.

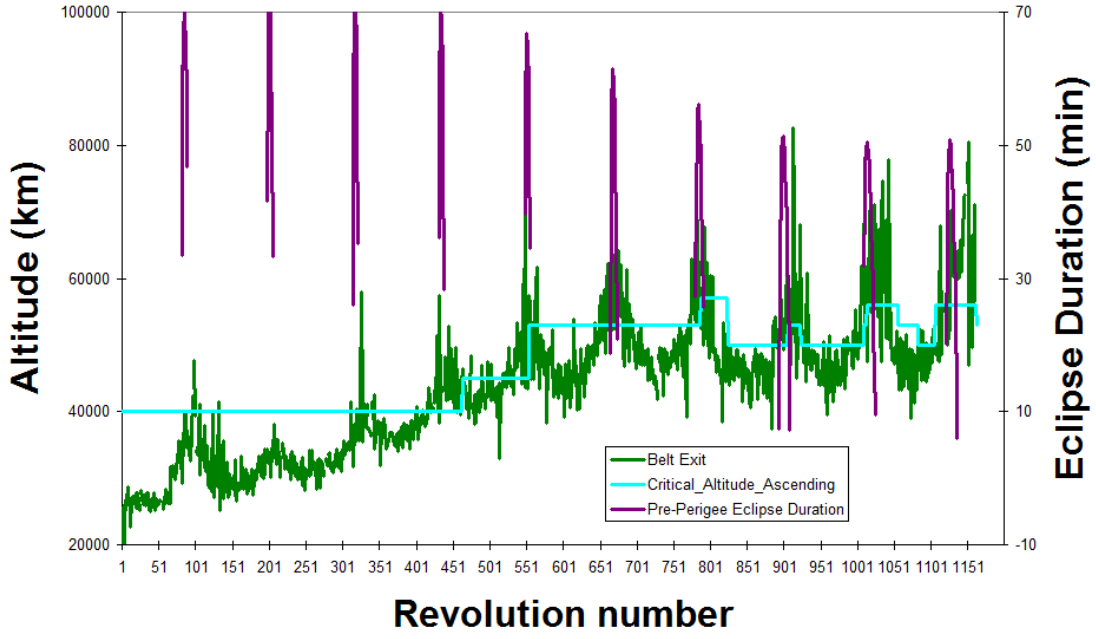

Fig. 6 Radiation belt exit with eclipse times and the "Critical Altitude Ascending"

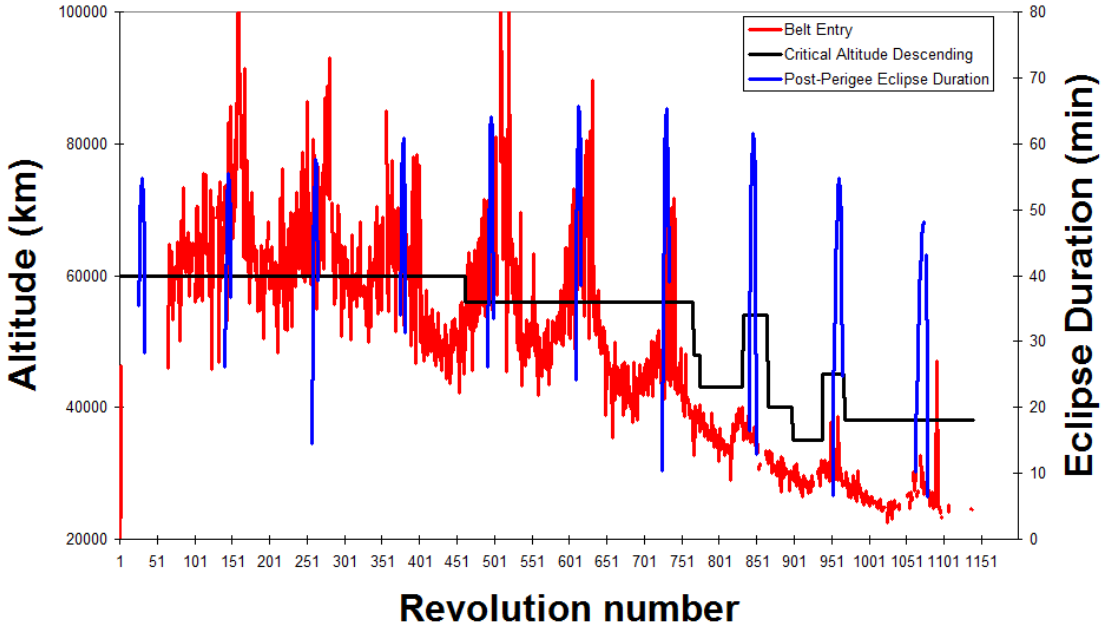

Fig. 7 Radiation belt entry with eclipse times and the "Critical Altitude Descending"

IV. Orbit Evolution

The other pronounced feature of figs. 2 & 3 is the trend of the belt entry altitude to reduce over time, whereas the belt exit altitude has increased. This is explained by the orbit evolution experienced by **Integral** since launch. As the line of apsides rotates, this affects the measured belt entry and exit altitudes. With an argument of perigee around 270°, the orbit is "upright", but as this value decreases, the belt exit altitude increases and, correspondingly, the belt entry altitude decreases. As an example, fig. 9 shows the belt entry and exit curves for revolution 1220 (left and right hand tracks respectively). Note the very low belt entry altitude, compared with that for the belt exit. However, it is expected from orbital perturbations that this evolution will reverse with time. Currently, (April 2012) the belt entry is deep within the cusp of the Earth's magnetosphere. Due to the nature of the orbit being an integral number of sidereal days, this cusp crossing will always be in the same place on the geoid.

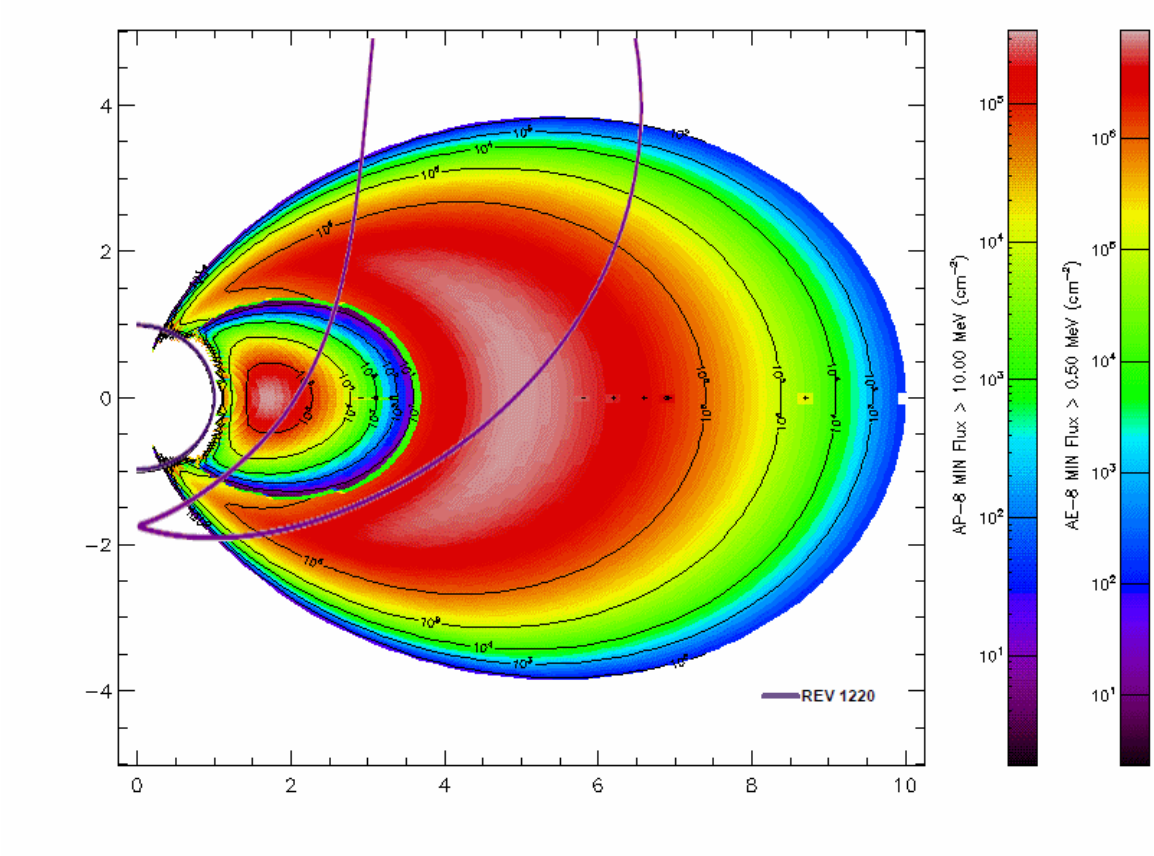

Fig. 9 'Fish-eye' plot showing a schematic of the belts entry and exit trajectories. Data from the AP8/AE8 programs (Vette, Sawyer and Vette).

At launch (17/10/2002), the **Integral orbit** had the following elements:

- Semi-major axis 86791.02 km
- Eccentricity 0.83252
- Inclination 52.17 deg
- Longitude of Ascending Node 103.29 deg

- Argument of Perigee 301.73 deg

This corresponds to an apogee height 153666.7km and a perigee height of 9059.3km with a period of 3 sidereal days. The first four graphs in fig. 10 show how the **relevant** orbital parameters evolved and are predicted to evolve. The plots show the actual evolution during Integral's lifetime and a prediction of their evolution to February 2021. Note that the inclination to the ecliptic is derived using inclination and longitude of ascending node and that the semi-major axis has not been included, as active orbital control is exercised to maintain the period to 3 sidereal days.

Thus, applying the geometry observed during the first 9 years of operations, it is expected that the effect of the proton belts will gradually reduce as the perigee height rises, reaching a minimum around December 2015. After that the perigee height falls again, and the proton counts will rise once more. This will continue until late 2020, after which orbital perturbations will again cause the perigee height to rise. The effect of the rotation of the line of apsides will mean that the Van Allen belt (electron and where appropriate proton) entry altitude will start to rise, reaching levels similar to those seen near the start of the mission. However, in compensation the belt exit altitude will reduce, maintaining science time. The orbit inclination w.r.t. the ecliptic will also oscillate considerably, but will remain high enough that the eclipse periods will remain seasonal and not extend over large parts of the year. Thus the times when Integral passes through the geotail will remain relatively short.

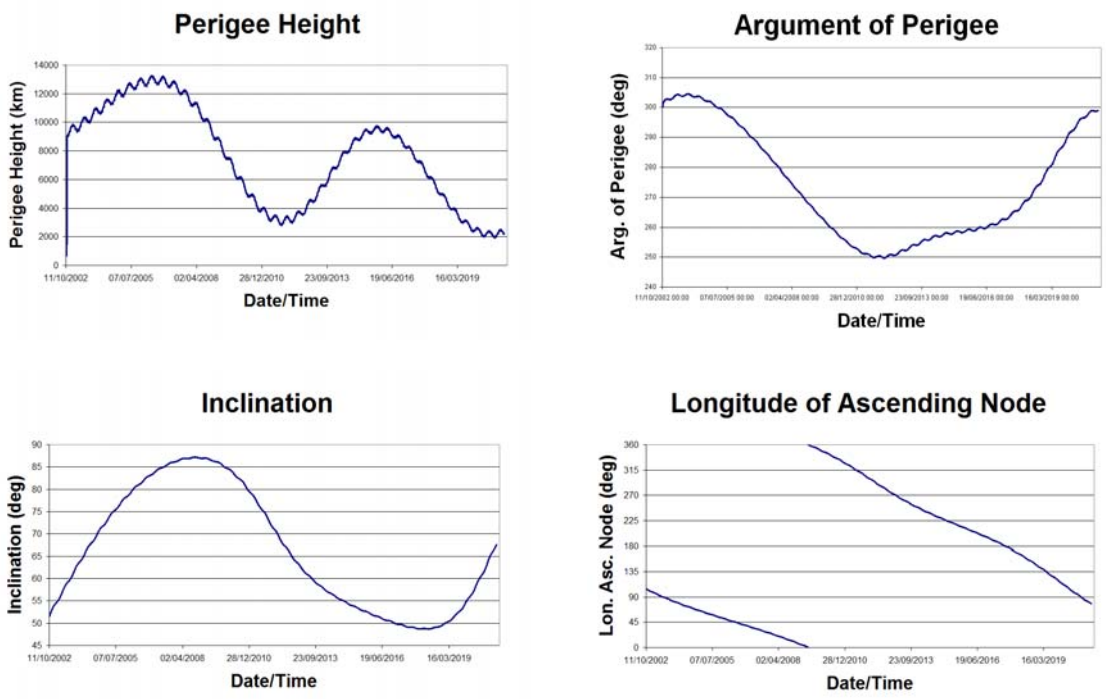

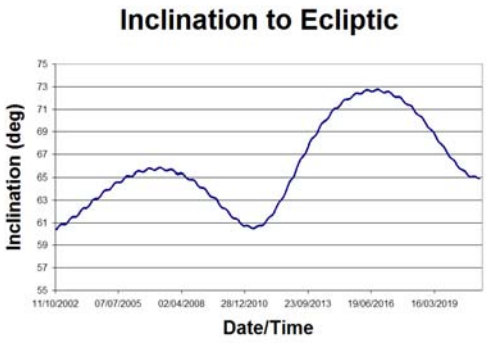

Figure. 10 Orbital Evolution

V. Solar Flares

In addition to the science operation restrictions due to Van Allen belt entry & exits, solar flares occasionally hinder science operations. Although these solar flares are an order of magnitude less intense than the radiation encountered during the Van Allen belt passage, they can still cause the instruments to automatically go to SAFE mode. This occurs with a frequency following the 11-year solar cycle. During the solar minimum it was a rare occurrence, whereas during the solar maximum about 10 a year would occur. A typical belt passage will cause the electron count to exceed 65535 **IREM** counts in 8 seconds and go off scale, whereas the peak of the most intense solar storm for 5 years reached only 11715 **IREM** counts, however with a much longer duration. It should also be noted that the proton belt, although more damaging than the electron belt, always lies within the latter. Therefore, the proton counts themselves are only rarely the limiting factor for instrument switch-off. When this occurs it is usually during the dissipation phase following a flare. For this study, however, such flares mask the belt entry and exit altitudes for that revolution. The effect of the solar cycle is to increase the frequency of such events, - the belts themselves seem to remain more or less unaffected. As an example Fig. 11 shows the radiation counts experienced during a solar flare where operations were interrupted for an entire orbit.

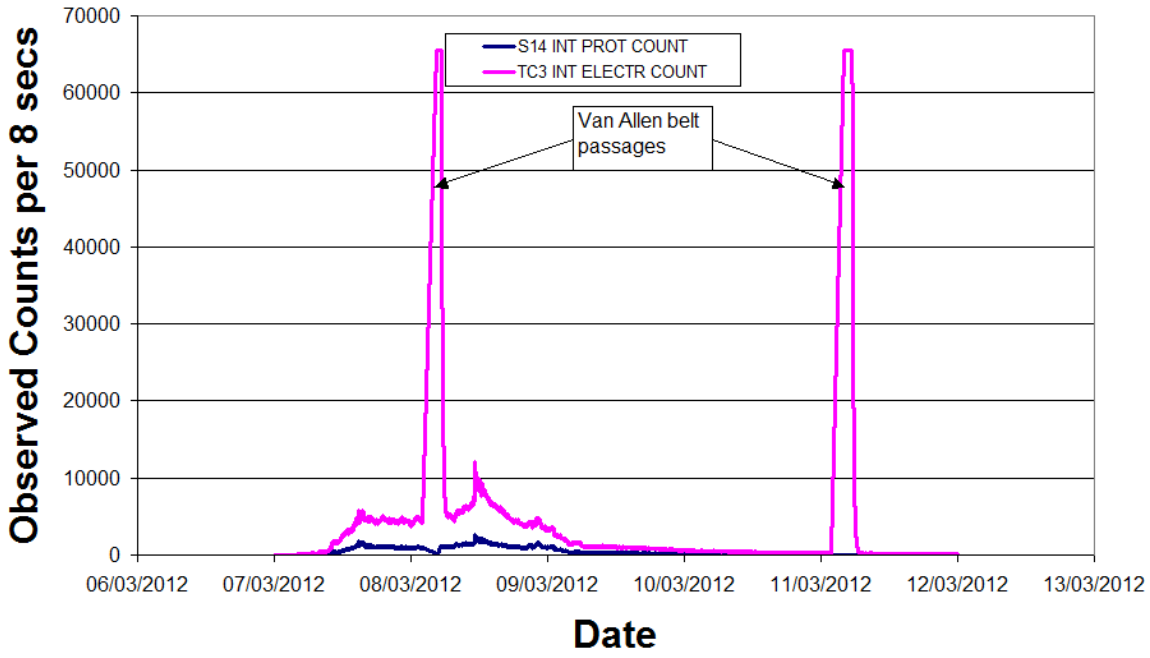

Fig. 11 Observed Radiation Levels during the Storm of 8/9 March 2012.

VI. Long term Predictions of Belt entry and exit altitudes

An initial evaluation of the future trend of the belt entry/exit altitudes was made based on the observations made since launch. The major component of this trend is the evolution of the argument of perigee, (perigee height does not contribute that much owing to the radial nature of the belts). By comparing the belt entry/exit altitude values observed earlier in the mission and projecting these forward using the argument of perigee as a reference, a prediction was prepared, see figures 12 & 13.

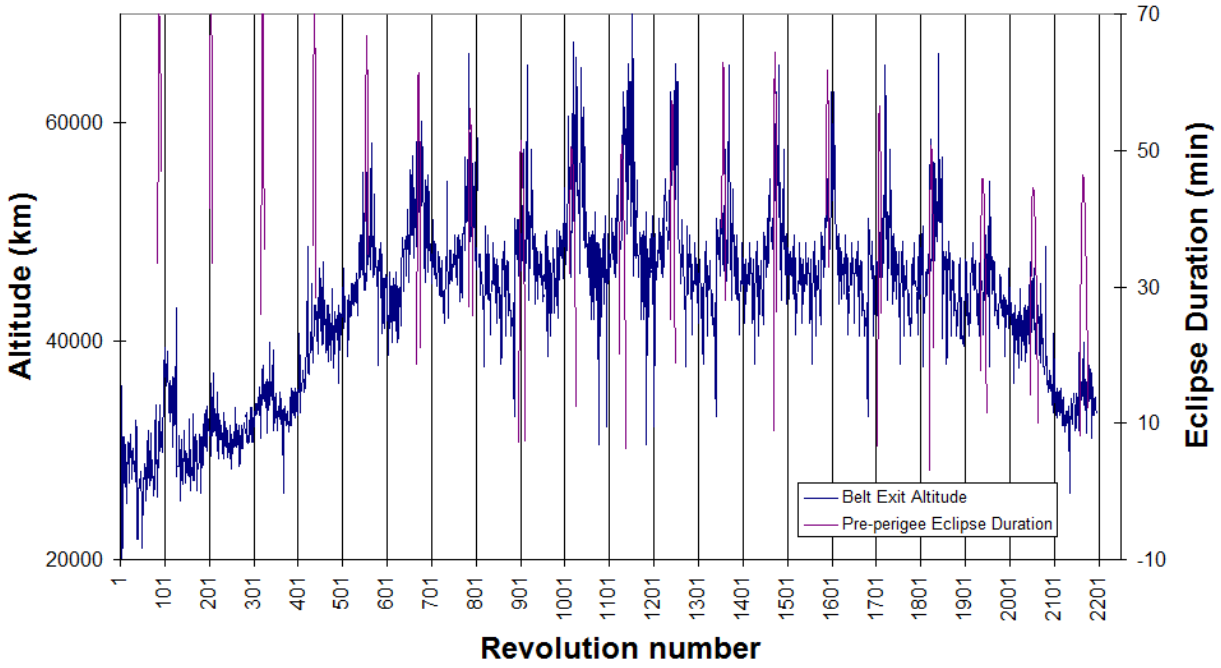

Fig. 12 Predicted evolution of the radiation belt exit altitude.

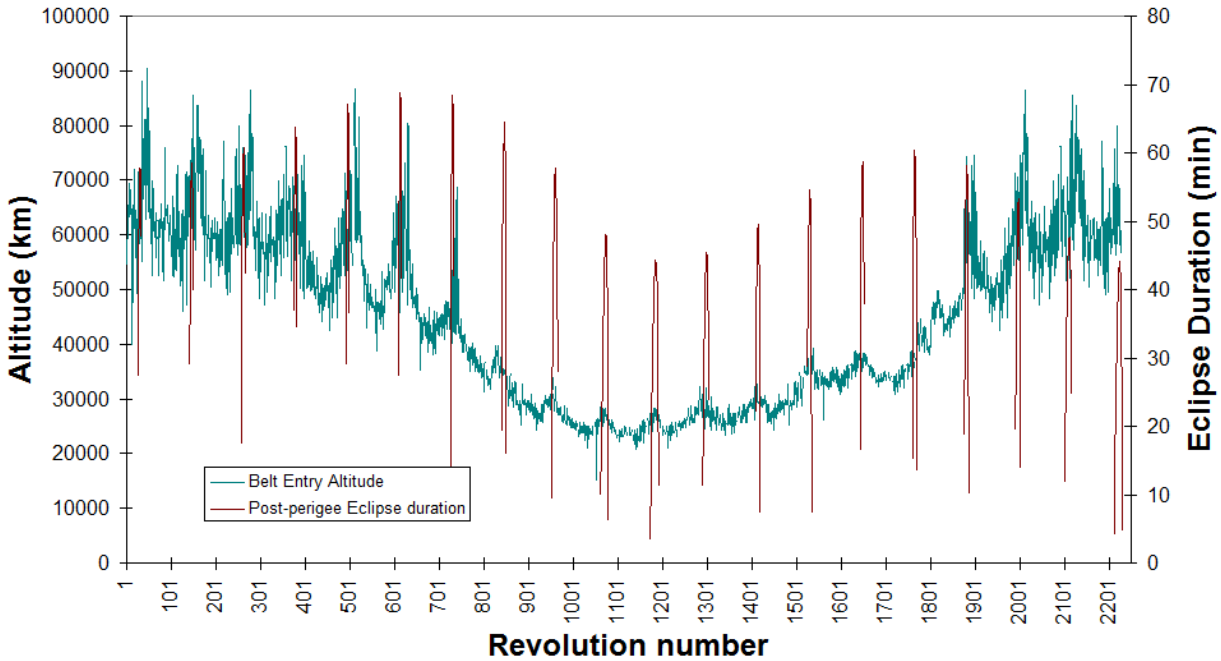

Fig. 13 Predicted evolution of the radiation belt entry altitude.

VII. Conclusion

By making use of the findings in this paper, Integral Science Operations have had a gain of up to 40 minutes science time per orbit. This was however, achieved during those periods of relatively low radiation at belt exits (that is not near the geotail).

They were not however applied at the radiation belt entries due to the operational requirement to provide adequate time for manual commanding should an instrument or spacecraft problem prevent the on-board systems from switching the instruments to safe mode.

The long-term prediction of the radiation belt entries and exits may provide assistance to strategic planning of the science operations into the future.

References

Alexeev I., Kalegaev V., "Global modeling of the magnetosphere in terms of paraboloid model of magnetospheric magnetic field"

Kalegaev V.V., Alexeev I.I., Feldstein Ya.I., "The geotail and ring current dynamics under disturbed conditions" Journal of Atmospheric and Solar-Terrestrial Physics Volume 63, Issue 5, March 2001.

Garrett, H. "Guide To Modeling Earth's Trapped Radiation Environment", AIAA G-083-1999

Sawyer, D. M., and Vette, J. I., "AP-8 Trapped Proton Environment for Solar Maximum and Solar Minimum," 76-06, NSSDC/WDC-A-R&S, 1976.

Vette, J. I., "The AE-8 Trapped Electron Model Environment," 91-24, NSSDC/WDC-A-R&S, 1991.

"Integral Science Data Centre" http://www.isdc.unige.ch/integral/

Stubbs T.J, et al. "Dawn-dusk asymmetry in particles of solar wind origin within the magnetosphere"

N. A. Tsyganenko, "A model of the near magnetosphere with a dawn-dusk asymmetry. 1. Mathematical structure", JOURNAL OF GEOPHYSICAL RESEARCH, VOL. 107, 1179, 15 PP., 2002

W. Hajdas, P. Buhler, C. Eggel, P. Favre, A. Mchedlishvili, A. Zehnder 'Radiation environment along the INTEGRAL orbit measured with the IREM monitor' Astron. Astrophys. 411:L43-L48,2003.

W.C. Blackwell, Jr., J.I. Minow, S.L. O'Dell, R.M. Suggs, D.A. Swartz, A.F. Tennant, S.N. Virani, and K.M. Warren, 'Modeling the Chandra Space Environment', Proc. SPIE Vol. 4140, p. 111-122, X-Ray and Gamma-Ray Instrumentation for Astronomy XI, Kathryn A. Flanagan; Oswald H. Siegmund; Eds. (2000)

S. L. O'Dell, M. W. Bautz, W. C. Blackwell, Y. M. Butt, R. A. Cameron, R. F. Elsner, M. S. Gussenhoven, J. J. Kolodziejczak, J. I. Minow, R. M. Suggs, D. A. Swartz, A. F. Tennant, S. N. Virani, and K. Warren, 'Radiation Environment of the Chandra X-ray Observatory' Proc. SPIE Vol. 4140, p. 99-110, X-Ray and Gamma-Ray Instrumentation for Astronomy XI, Kathryn A. Flanagan; Oswald H. Siegmund; Eds (2000)